Comparison of Triaxial Characterization of Road Materials for Highway Structural Modelling

Rielle Haichert P.Eng.
Vice President Engineering
PSI Technologies Inc.
Saskatoon, SK
rhaichert@pavesci.com

Curtis Berthelot, Ph.D., P.Eng.
President & Chief Technical Officer
PSI Technologies Inc.
Saskatoon, SK
cberthelot@pavesci.com

Jody Berthelot, E.I.T.
General Manager
PSI Technologies Inc.
Saskatoon, SK
jberthelot@pavesci.com

Steven Li, E.I.T.
Project Manager
PSI Technologies Inc.
Saskatoon, SK
sli@pavesci.com

Paper prepared for
SO - Innovation in Roadway/Embankment Materials and Geotechnical Engineering
2026 Transportation Association of Canada (TAC) Conference & Exhibition
Winnipeg, Manitoba

Abstract

Material constitutive relations are an essential input of mechanistic modelling. However, road material properties are complex in that they are highly sensitive to the field state conditions upon which they are placed. Road materials therefore need to be characterized across the full spectrum of field state conditions. Full spectra characterization is required to reliably quantify road structural primary response and predict life cycle structural performance prediction of road assets.

This paper compares the use of AASHTO T307 single frequency and PSI*Materials*4D triaxial non-linear multi-frequency sweep characterization of typical flexible pavement materials within a primary pavement road structure. These material constitutive properties were encoded in a three-dimensional numerical modelling package PSI*Pave*3D to predict the structural behaviour of a typical primary rural flexible pavement structure under heavy truck loading.

This study showed the AASHTO T307 material testing protocols are limited to quantify accurate material constitutive behavior across typical Canadian field state conditions. The PSI*Materials*4D non-linear complex modulus triaxial frequency sweep characterization was found to provide more realistic material properties across all field state conditions, pavement structure types and material properties required for mechanistic road modelling. As a result, PSI*Materials*4D was found to provide more realistic 3D pavement primary responses profiles when encoded into an advanced numerical mechanistic road model. This was particularly the case in terms of principal shear strain propagation within the pavement system which is the dominant mode of structural failure in a flexible pavement. Full frequency sweep material property profiles within PSI*Materials*4D also enables characterization of the effects of moisture, slower moving traffic, turning, braking and accelerating load scenarios, particularly common in heavy industry as well as urban pavements.

Introduction

Material constitutive relations are an essential input of mechanistic modelling. Accurate continuum mechanics pavement materials characterization is critical for pavement structural analysis purposes within a mechanistic framework. However, continuum mechanistic road material characterization is complicated as it must accurately represent *in situ* field state stress and strain state, load rate, and climatic conditions of the material 3D as is in the road structure.

Objective and Scope

The primary objective of this study was to compare AASHTO T307 (1,2,3,4) material characterization protocols to PSI*Materials*4D non-linear triaxial frequency sweep mechanistic material constitutive characterization (5). The second objective of this study was to evaluate the end resultant primary response profiles resulting from both material constitutive relation inputs obtained into a three-dimensional numerical road model PSI*Pave*3D (6). Principal shear strains and vertical deflection profiles with depth into a typical primary flexible pavement structure under primary weights and dimensions of B-train loading were evaluated.

Material Selection and Continuum Sample Preparation

Engineers have developed material selection guidelines and testing protocols for asphaltic bound hot mix materials, unbound granular materials, and soils based on physical properties such as grain size distribution, mix volumetrics, plasticity of fines, fines content, particle fracture, moisture-density densification, etc. As well, road materials have been characterized using empirical mechanical tests such as marshall stability and flow, California bearing ratio, unconfined compressive and tensile strength tests.

This study investigated two alternate mechanistic based material preparation and characterization methodologies to characterize the continuum material constitutive properties of granular materials using; AASHTO T307 and PSI*Materials*4D characterization protocols for use in mechanistic pavement analysis. The material constitutive properties obtained were entered into a 3D numerical road model PSI*Pave*3D to evaluate and compare the road structural primary responses under typical B-train loading at primary weight limits.

As seen in Figure 1, SMHI Type 33 unbound granular base, SMHI Type 8 subbase and USCS SC subgrade materials considered in this study were chosen to meet grain size specification (and other properties) of typical flexible pavement road substructure materials. Standard Proctor compaction protocols were used to determine optimum density and moisture contents of the granular and subgrade samples. Samples used in this study were prepared at standard proctor optimum moisture and density, as shown in Figure 1.

AASHTO T307 sample preparation protocols employ a 150mm x 300mm sample geometry compacted using vibratory compaction in five uniform layers. The sample dimensions and layered compaction protocols of AASHTO T307 resulted in samples that are not a continuum sample for mechanistic characterization.

PSI*Materials*4D triaxial frequency sweep mechanistic characterization protocols utilizes a 150mm x 150mm gyratory compacted continuum sample at gyratory settings that provide optimal target densification of the materials using full feedback control to the precise end product density specified. The PSI*Materials*4D sample preparation protocol also provides a true continuum non-layered sample at a specific density more representative of that constructed in the field.

Figure 1. Grain Size Distribution Specification and Standard Proctor Moisture-Density of Base, Subbase and Subgrade Considered in this Study

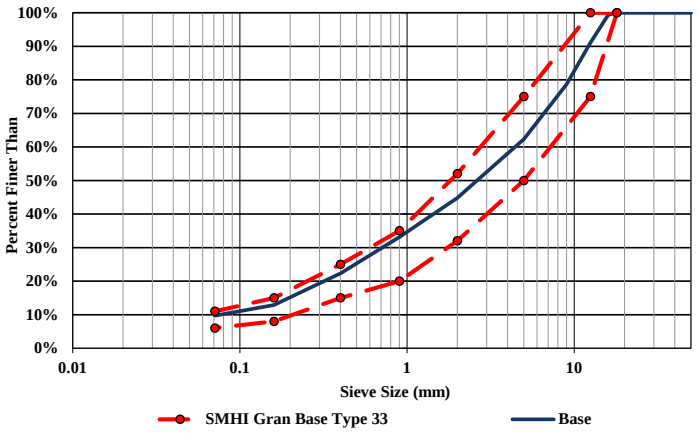

Base – Grain Size Distribution

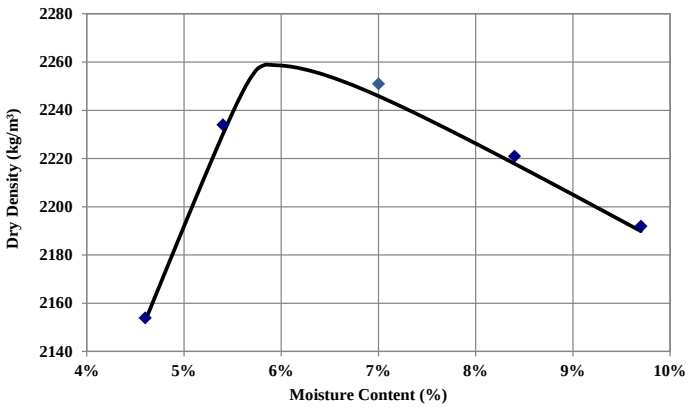

Base – Standard Moisture Density

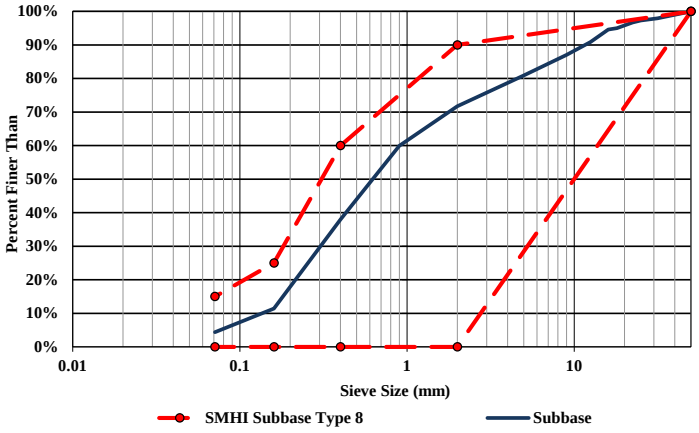

Subbase – Grain Size Distribution

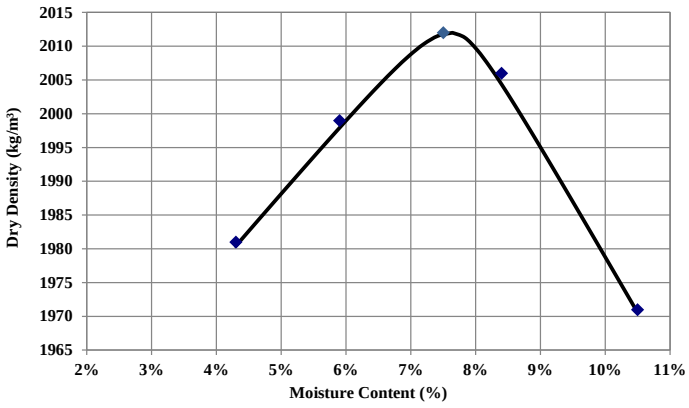

Subbase – Standard Moisture Density

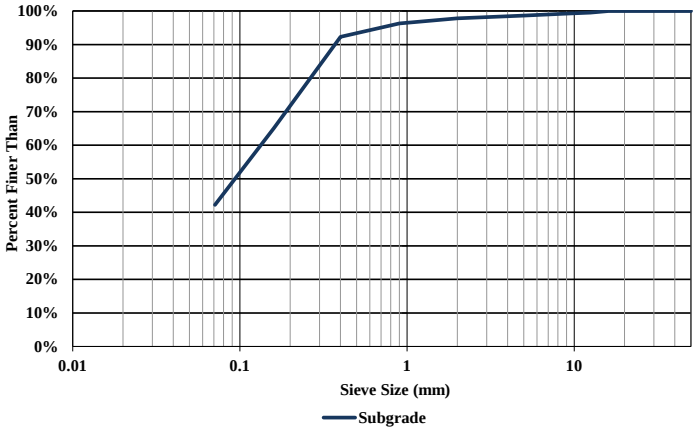

Subgrade – Grain Size Distribution

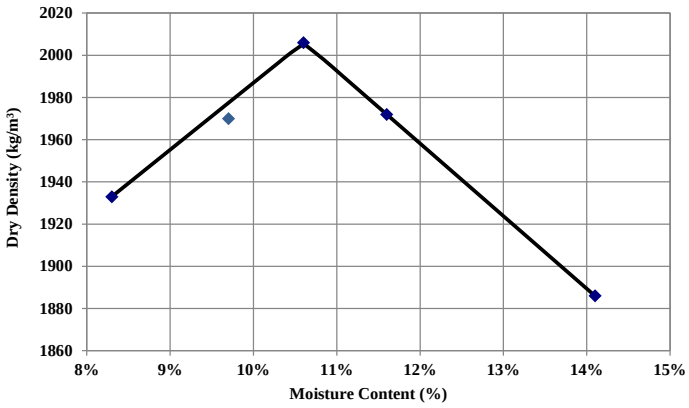

Subgrade – Standard Moisture Density

AASHTO T307 and PSI*Materials*4D Triaxial Dynamic Material Characterization

Triaxial dynamic characterization of asphalt concrete, unbound granular base, subbase and subgrade materials was performed to obtain material constitutive behaviour profiles required for 3D road structural primary response modelling. The AASHTO T307 and PSI*Materials*4D triaxial test frames are illustrated in Figure 2 a) and b), respectively. The PSI*Materials*4D test apparatus was used to characterize the asphaltic concrete mix as well as the granulars and soils because the AASHTO T307 apparatus and protocols could only characterize granulars and soils.

Figure 2. AASHTO T307 and PSI*Materials*4D Triaxial Sample Characterization Apparatus

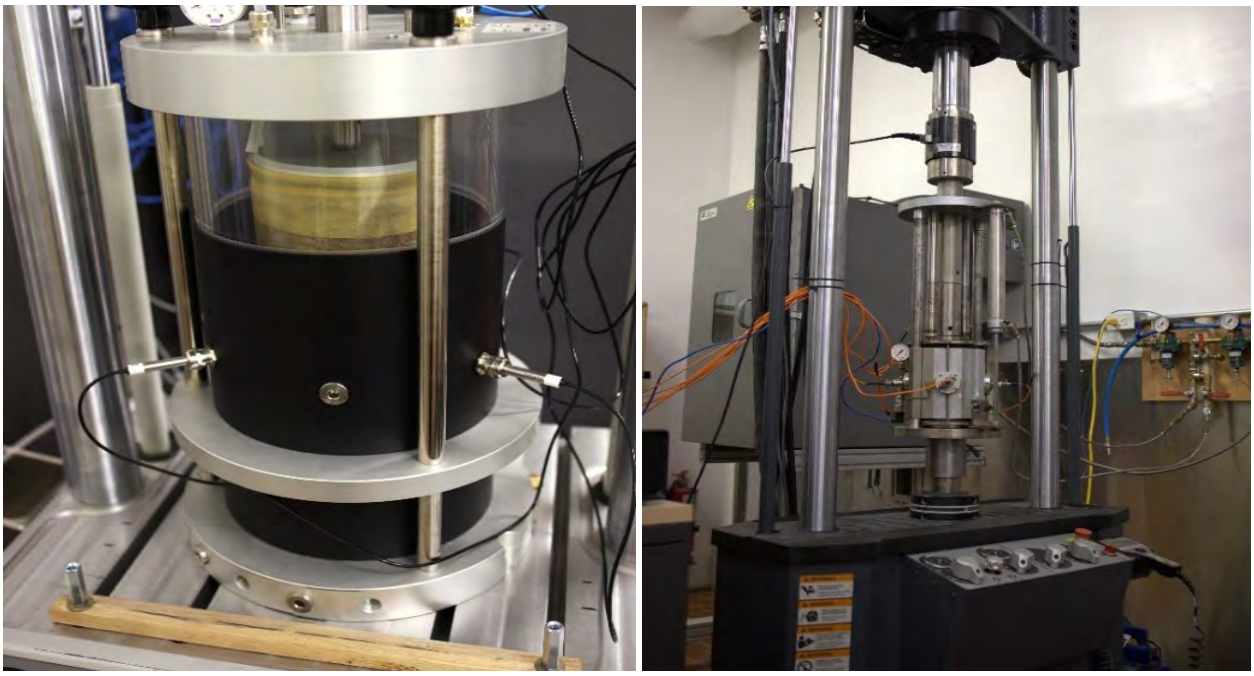

a) AASHTO T307 b) PSI*Materials*4D

Figure 3 and Figure 4 illustrate the stress states applied in both the AASHTO T307 and PSI*Materials*4D triaxial testing protocols, respectively. AASHTO T307 test protocols for granular materials specify a 0.l sec haversine load pulse at 10 Hz frequency with a 0.9 sec rest between load pulses. As seen in Figure 3, the range of 3D stress states for AASHTO T307 triaxial characterization protocols employs is 15 independent test conditions for granular base, subbase and subgrade materials. The peak octahedral shear stress and octahedral normal stress for base and subbase in the AASHTO T307 test protocol is 120 kPa and 215 kPa, respectively. For subgrade materials the peak octahedral shear stress and octahedral normal stress specified by AASHTO T307 protocol is 40 kPa and 75 kPa, respectively.

As seen in Figure 4, PSI*Materials*4D material constitutive characterization protocols employ a wider range of testing stress states (25 independent stress states) and applies the stresses across 0.1 to 10 Hz sinusoidal load waveform in a frequency sweep. The PSI*Materials*4D stress states are also applied in continuous positive as well as an additional 5 independent fully reversed stress states (ie. positive and negative cyclical deviatoric stresses with respect to the sample axial coordinate direction) to account for tensile stresses generated under moving traffic loading within the surfacing layers.

Figure 3. AASHTO T307 Stress State Characterization

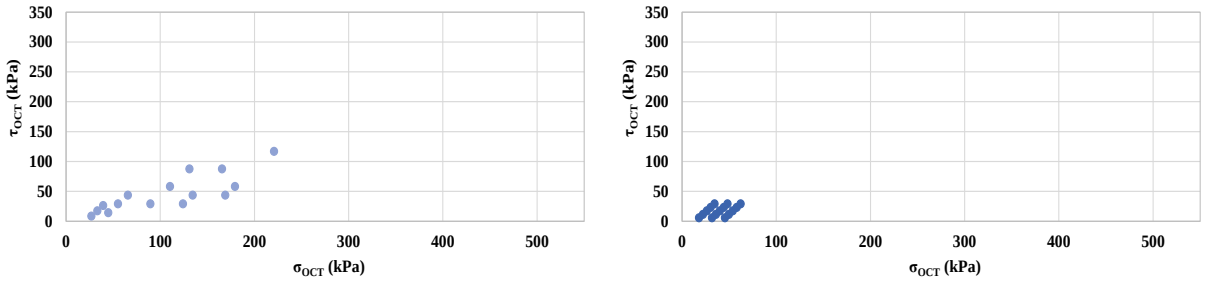

a) Base/Subbase b) Subgrade

Figure 4. PSI*Materials*4D Stress State Characterization

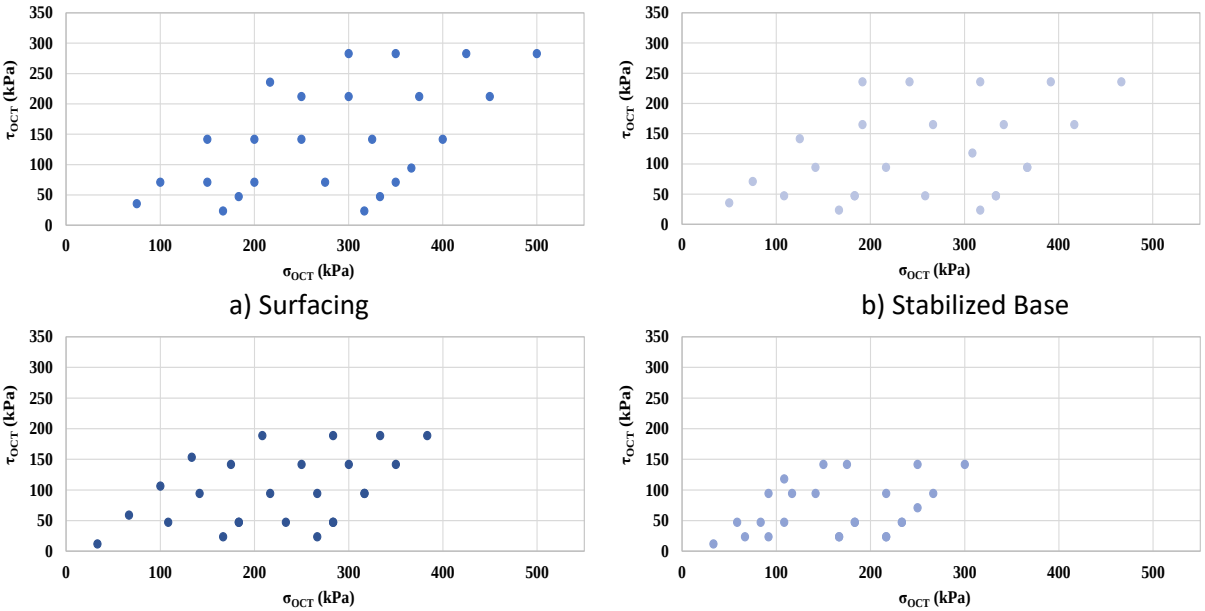

a) Surfacing b) Stabilized Base

c) Base d) Subbase

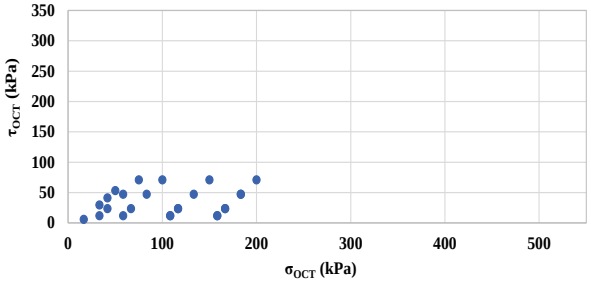

e) Subgrade

The possible 125 PSI*Materials*4D triaxial frequency sweep loading conditions were developed to more fully account for all potential field state effects of traffic load speed, braking, turning, dynamic loadings, as well as moisture state as typically experienced under heavy truck loadings within a feedback controlled modelling framework in rural as well as urban field state conditions, as illustrated in Figure 5. PSI*Pave*3D can also model both rural and urban pavement cross sections of various user defined cross sectional dimensions.

Figure 5. PSI*Materials*4D Triaxial Feedback Controlled Frequency Sweep Characterization under B-Train Loading Illustration

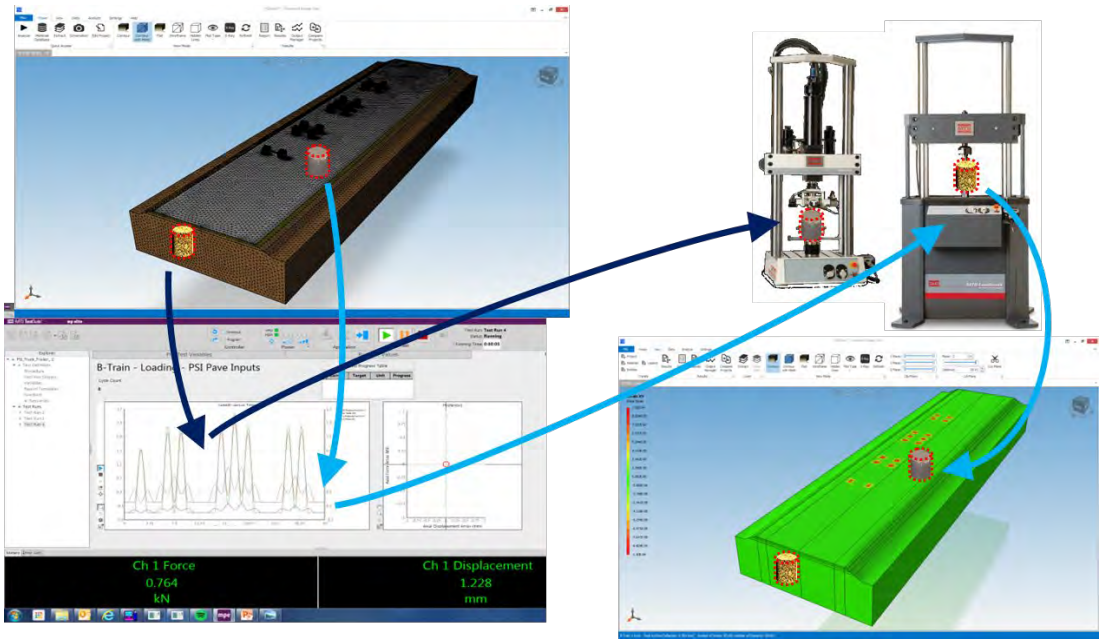

As illustrated in Figure 5, PSI*Pave*3D non-linear computational road modelling can iteratively repeat the modelling cycle until the non-linear material properties converge onto a numerical backcalculated solution of laboratory specified material property for that specific pavement design, loadings and geometry.

Figure 6 illustrates the triaxial material constitutive properties for a standard Type 1 hot mix asphalt concrete commonly used to surface primary flexible pavements. Material properties are presented across load frequency and with respect to orthogonal and shear octahedral stress state to cover the full range of non-linear behaviour. Only PSI*Materials*4D test regime was used in this study for PSI*Pave*3D modelling purposes.

Figure 7 through Figure 12 illustrates the triaxial material constitutive properties obtained from both AASHTO T307 and PSI*Materials*4D material characterization protocols plotted on the same scale range for ease of comparison. The material properties in PSI*Materials*4D are presented at five frequencies, 0.1 Hz load frequency up to 10 Hz load frequency whereas the material properties presented from the AASHTO T307 were only tested at 10 Hz load frequency. As seen in Figure 7 through Figure 12, there was a significant difference between the material constitutive properties and the field state stress range utilized with AASHTO T307 and PSI*Materials*4D characterization protocols. The dynamic modulus, shear modulus and Poisson's ratio of the granular base, subbase and subgrade obtained by AASHTO T307 was found to be significantly lower (up to 75 percent lower) relative to that obtained from PSI*Materials*4D.

The material property results are presented with respect to octahedral orthogonal and shear stress states. It should be noted that AASHTO T307 does not specify a test protocol for asphaltic concrete. Therefore, only PSI*Materials*4D asphalt concrete fully reversed triaxial frequency sweep characterization was performed on the hot mix asphaltic surfacing. Since there is no comparison with AASHTO T307, the PSI*Materials*4D material constitutive relations of the hot mix asphalt concrete were used herein.

Figure 6. PSI*Materials*4D Dynamic Modulus, Shear Modulus and Poisson's Ratio of Typical Type 1 Hot Mix Asphalt Concrete

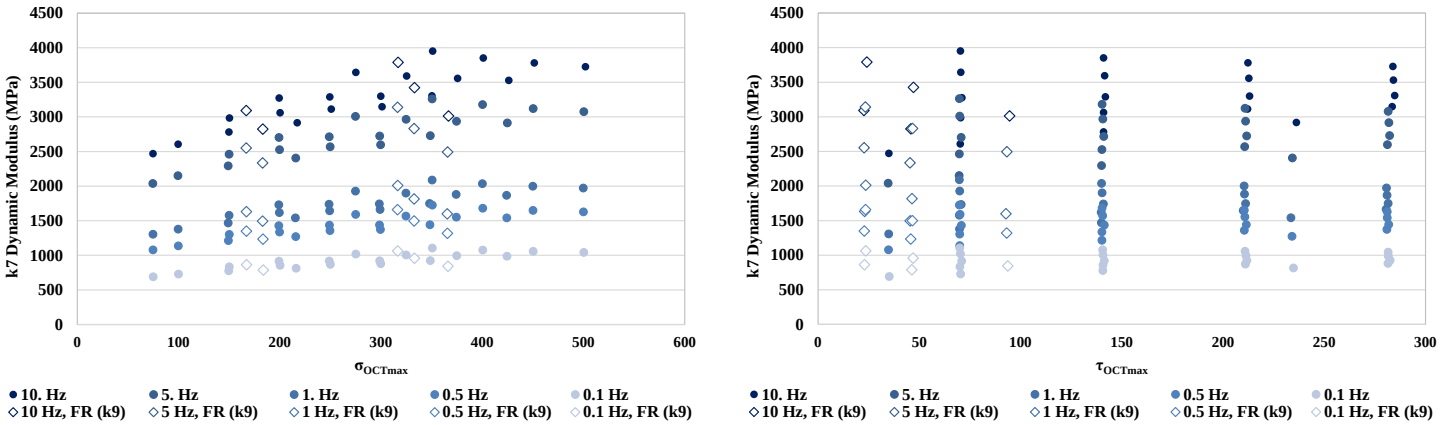

Dynamic Modulus (*PSIMaterials4D*)

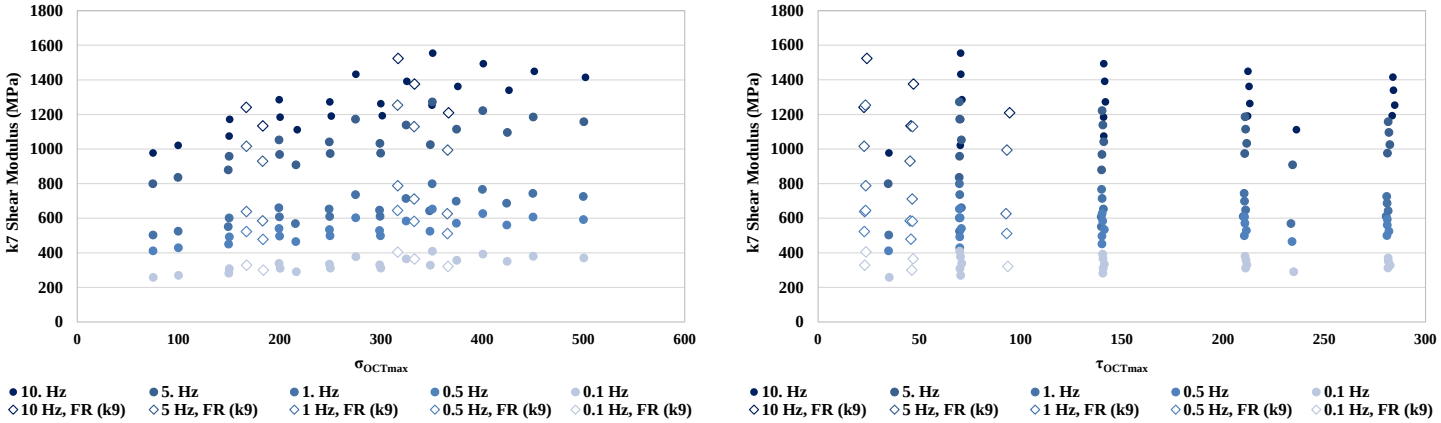

Shear Modulus (*PSIMaterials4D*)

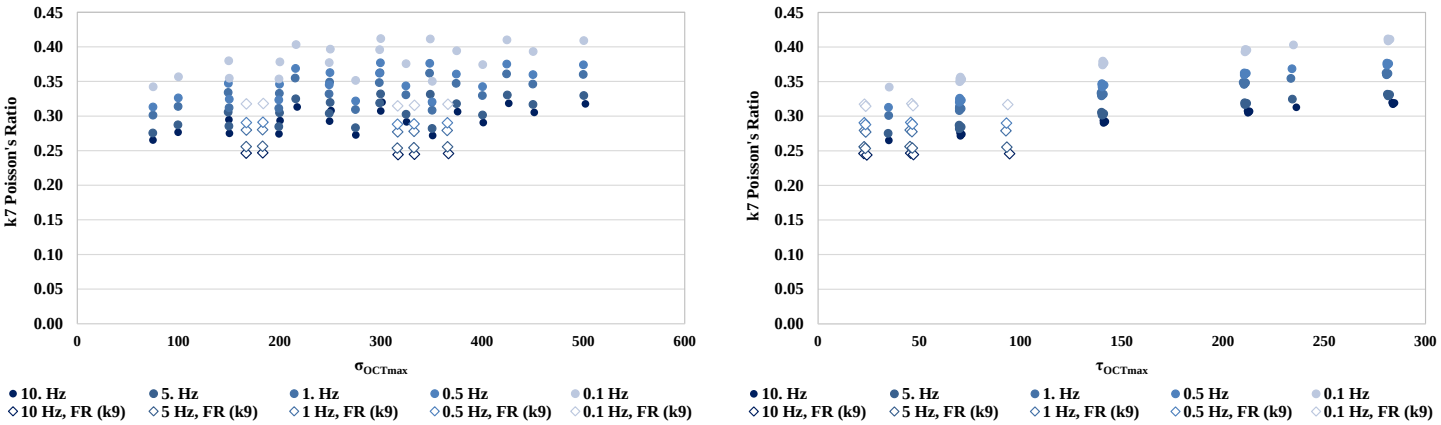

Poisson's Ratio (*PSIMaterials4D*)

Figure 7. Dynamic Modulus across Octahedral Normal Stress States and Load Frequencies

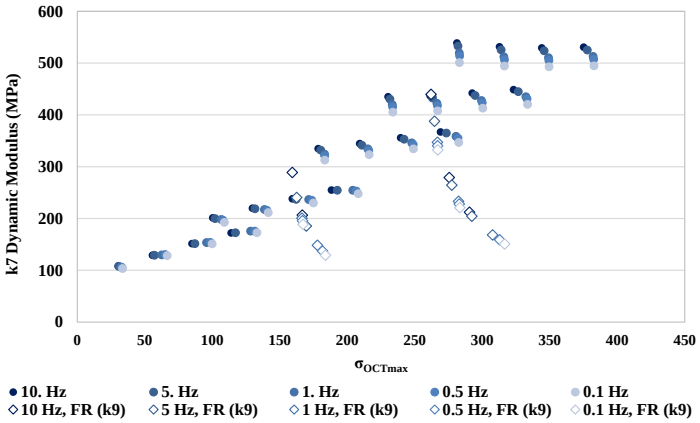

Base (PSI*Materials*4D)

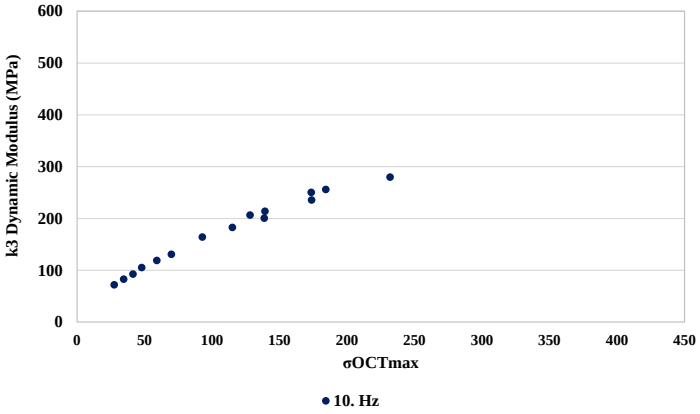

Base (AASHTO T307)

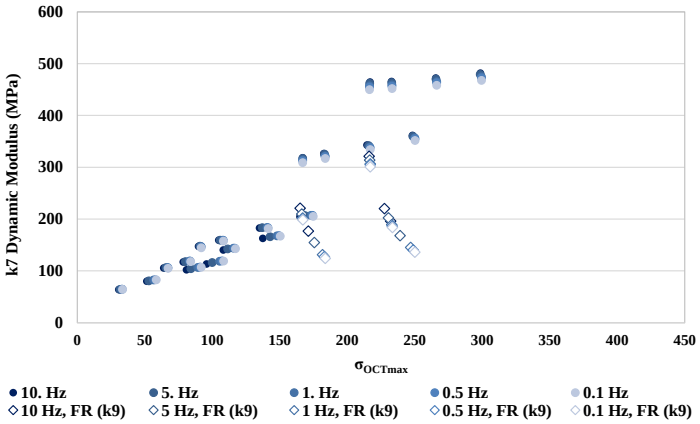

Subbase (PSI*Materials*4D)

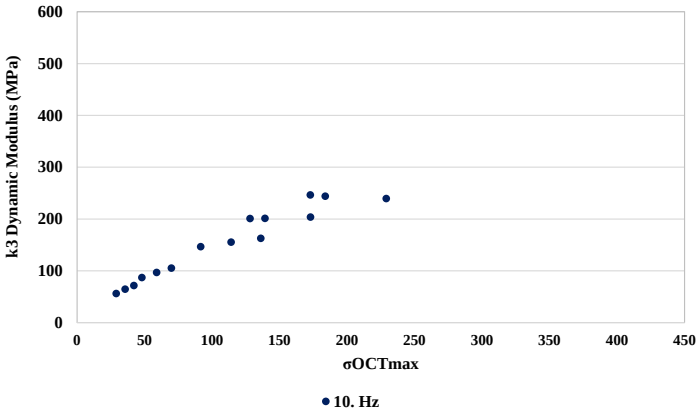

Subbase (AASHTO T307)

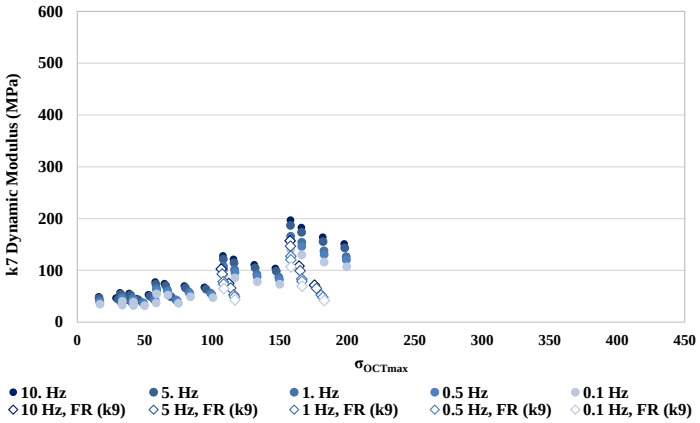

Subgrade (PSI*Materials*4D)

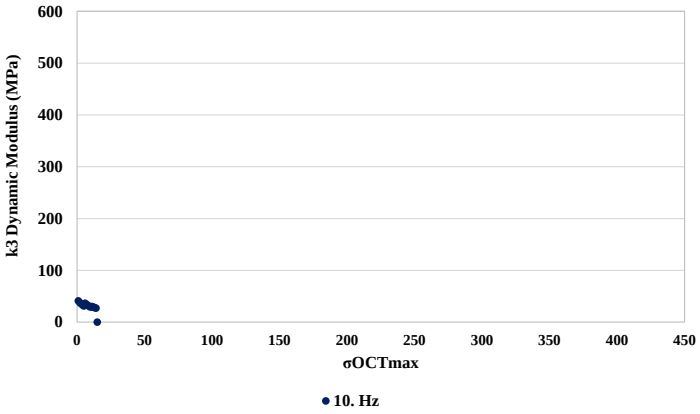

Subgrade (AASHTO T307)

Figure 8. Dynamic Modulus across Octahedral Shear Stress States and Load Frequencies

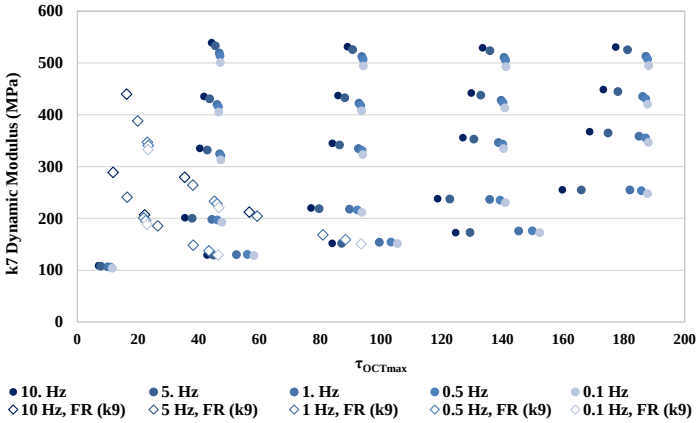

Base (PSI*Materials*4D)

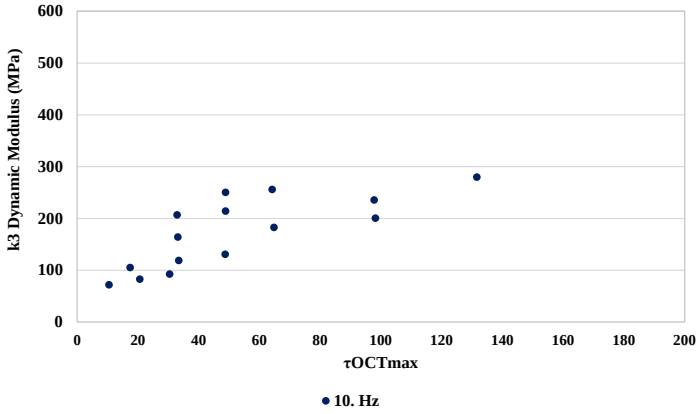

Base (AASHTO T307)

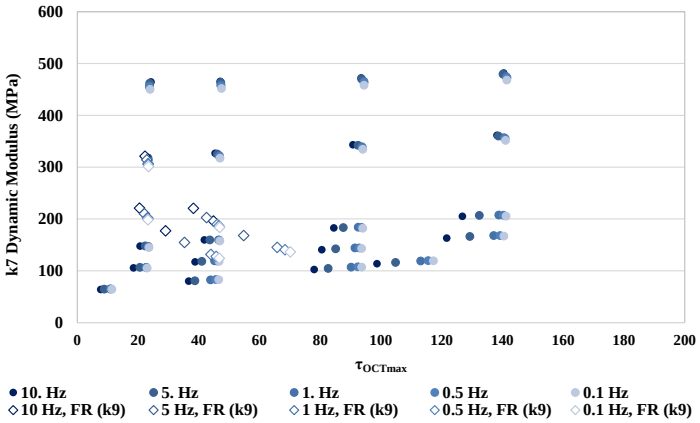

Subbase (PSI*Materials*4D)

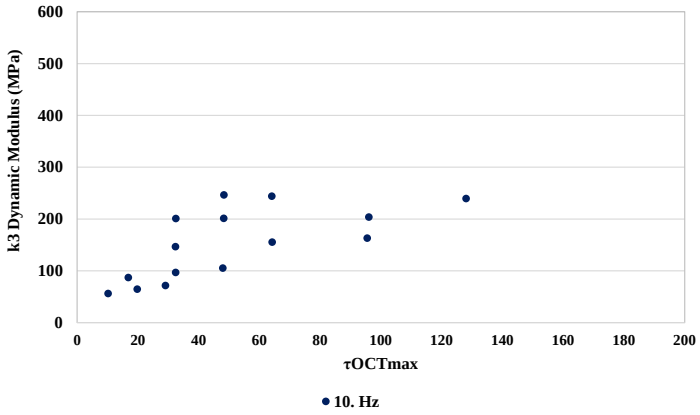

Subbase (AASHTO T307)

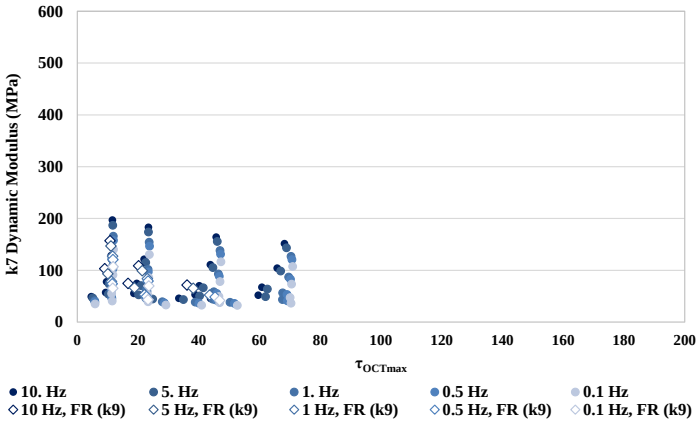

Subgrade (PSI*Materials*4D)

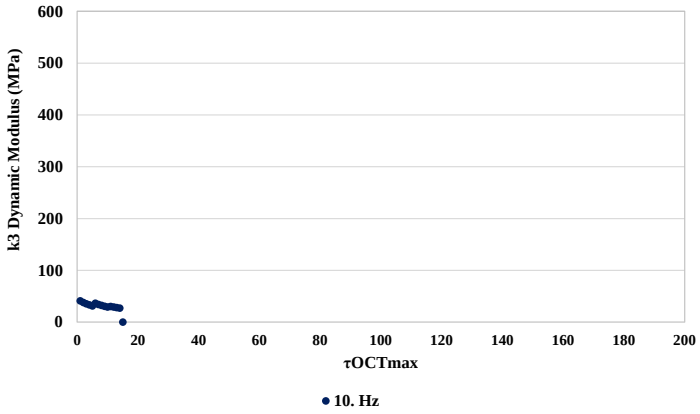

Subgrade (AASHTO T307)

Figure 9. Shear Modulus across Octahedral Normal Stress States and Load Frequencies

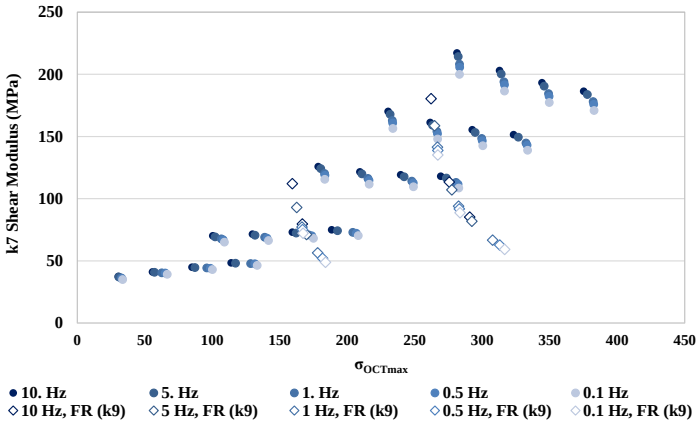

Base (PSI*Materials*4D)

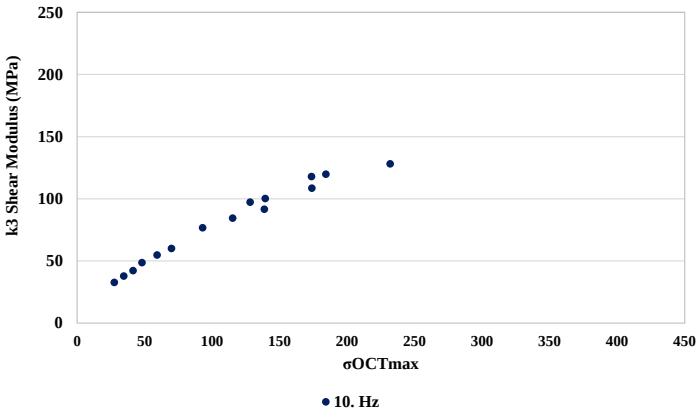

Base (AASHTO T307)

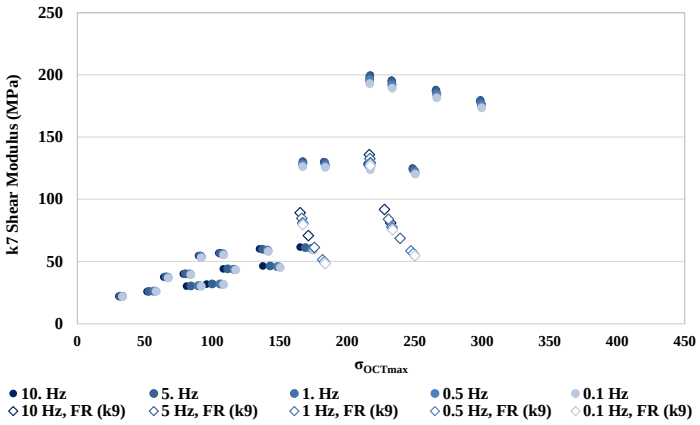

Subbase (PSI*Materials*4D)

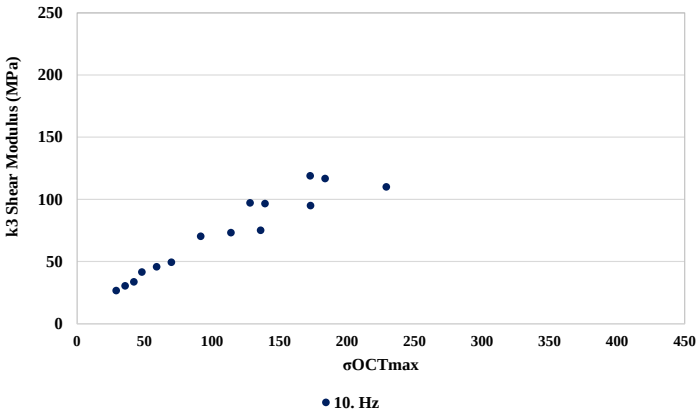

Subbase (AASHTO T307)

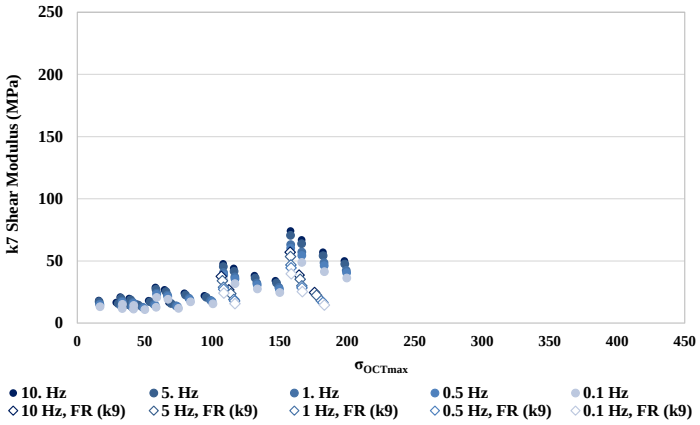

Subgrade (PSI*Materials*4D)

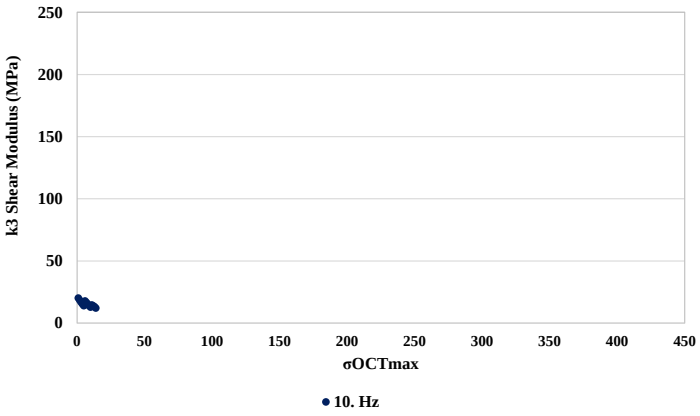

Subgrade (AASHTO T307)

Figure 10. Shear Modulus across Octahedral Shear Stress States and Load Frequencies

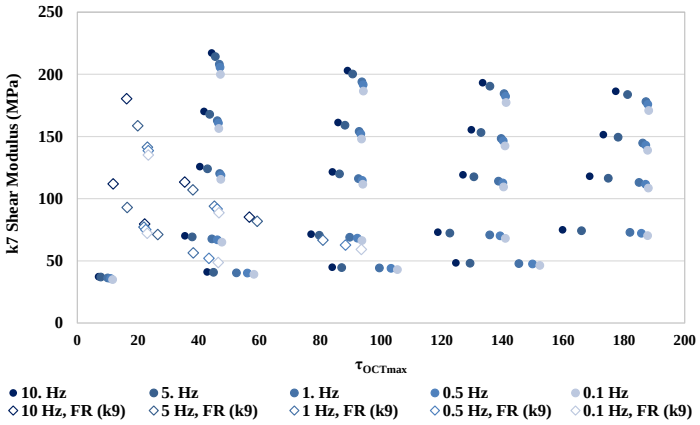

Base (PSI*Materials*4D)

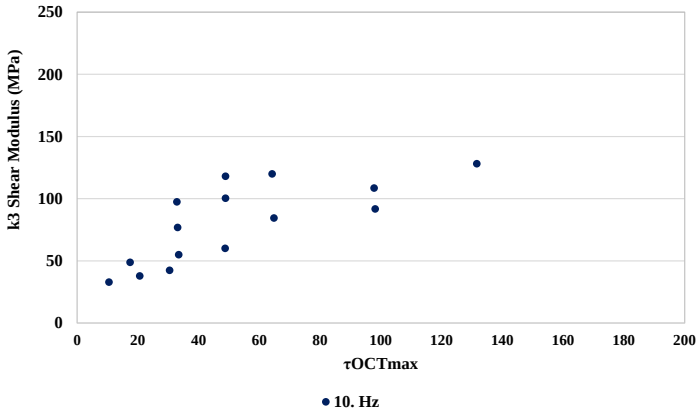

Base (AASHTO T307)

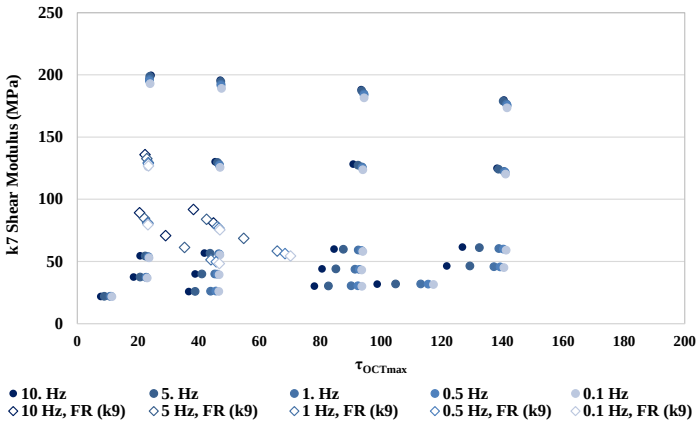

Subbase (PSI*Materials*4D)

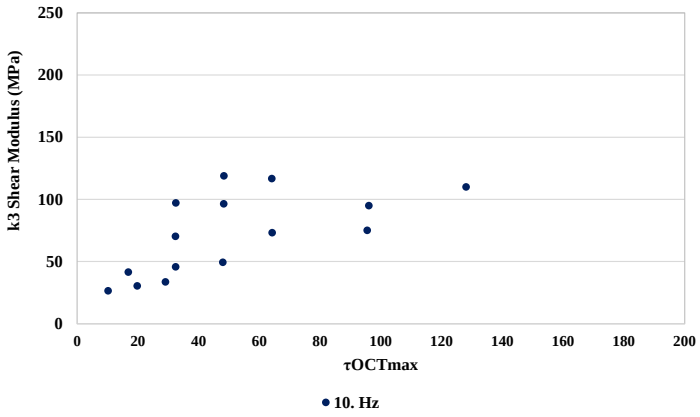

Subbase (AASHTO T307)

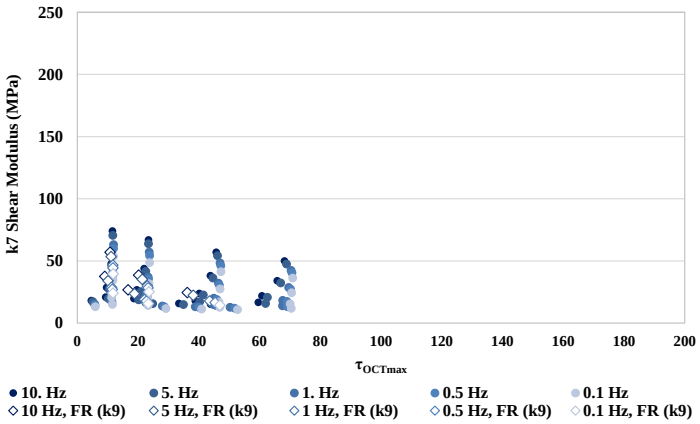

Subgrade (PSI*Materials*4D)

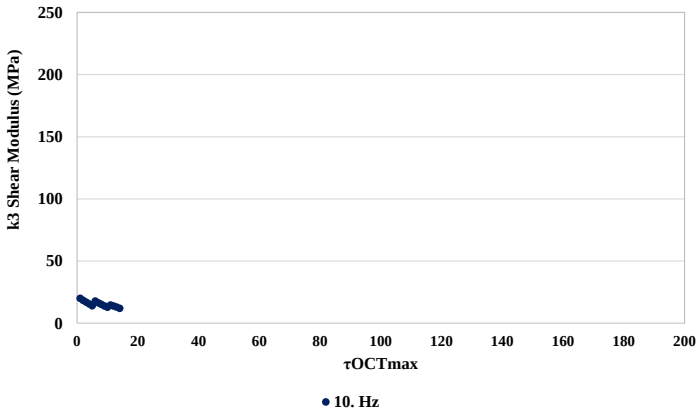

Subgrade (AASHTO T307)

Figure 11. Poisson's Ratio across Octahedral Normal Stress States and Load Frequencies

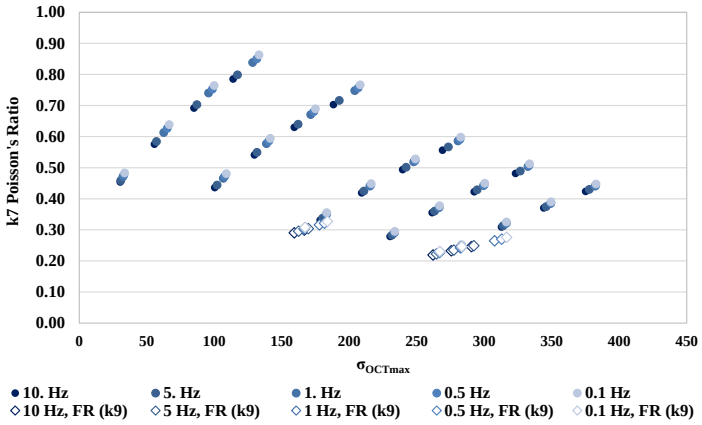

Base (PSI*Materials*4D)

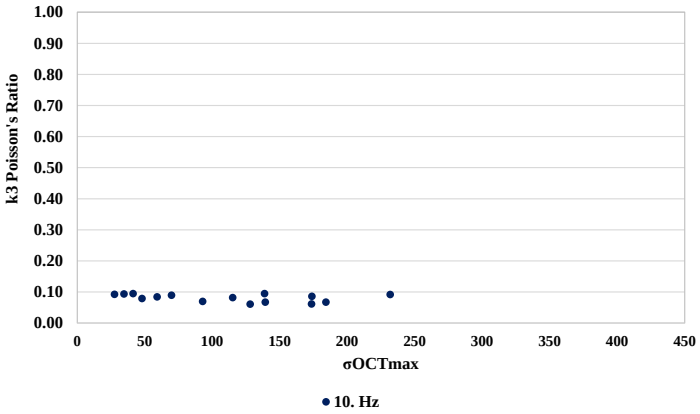

Base (AASHTO T307)

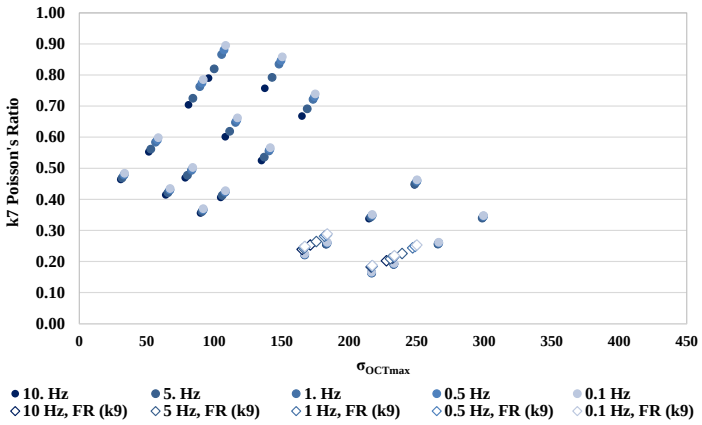

Subbase (PSI*Materials*4D)

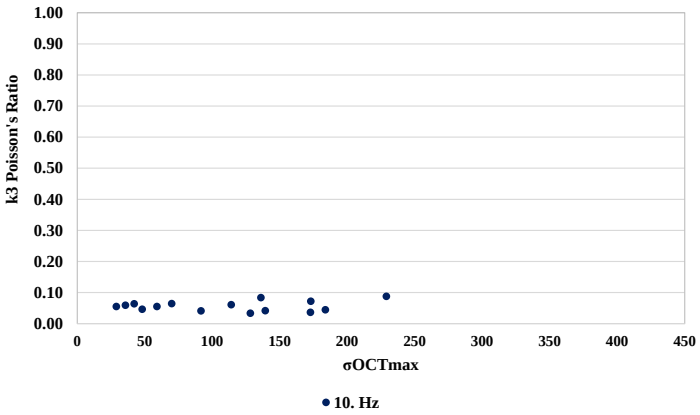

Subbase (AASHTO T307)

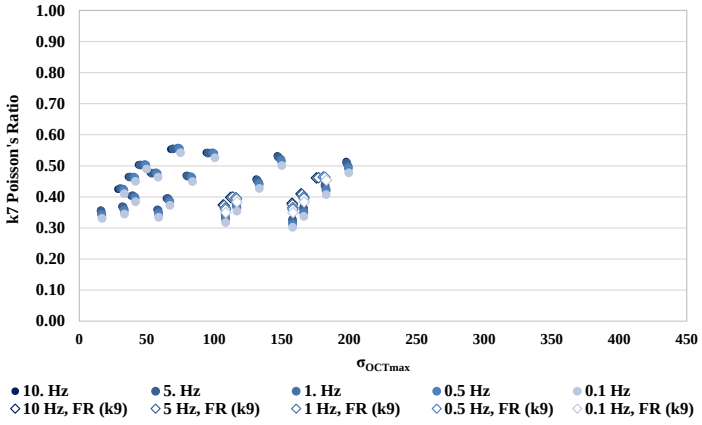

Subgrade (PSI*Materials*4D)

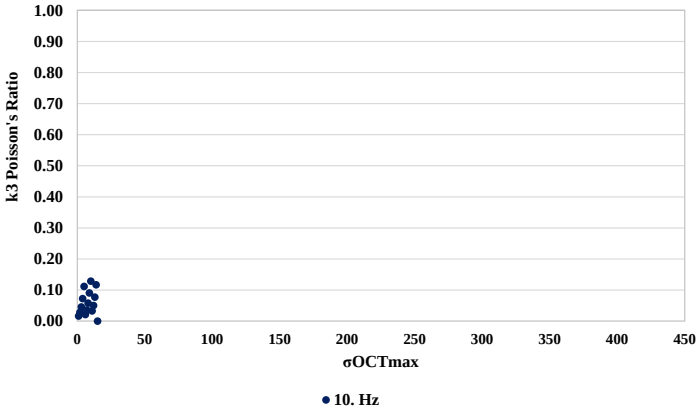

Subgrade (AASHTO T307)

Figure 12. Poisson's Ratio across Octahedral Shear Stress States and Load Frequencies

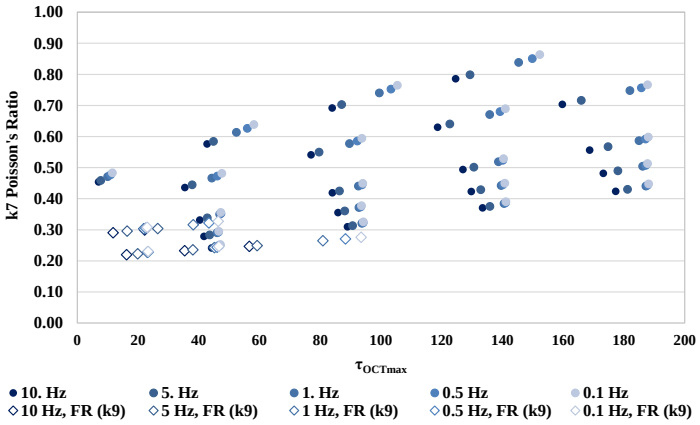

Base (PSI*Materials*4D)

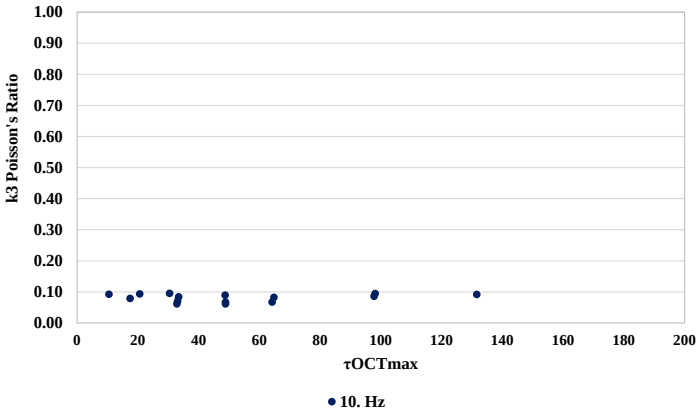

Base (AASHTO T307)

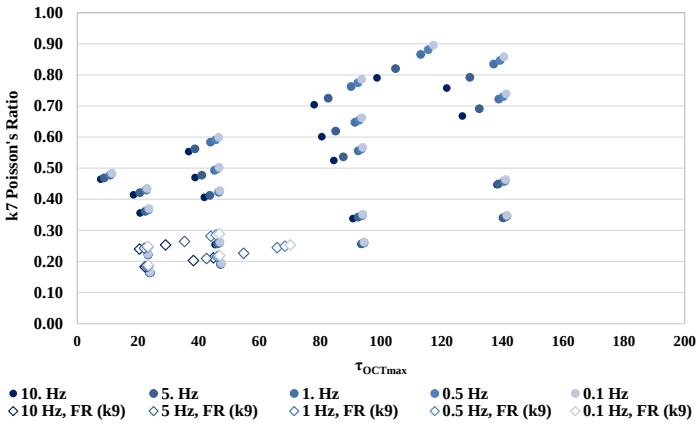

Subbase (PSI*Materials*4D)

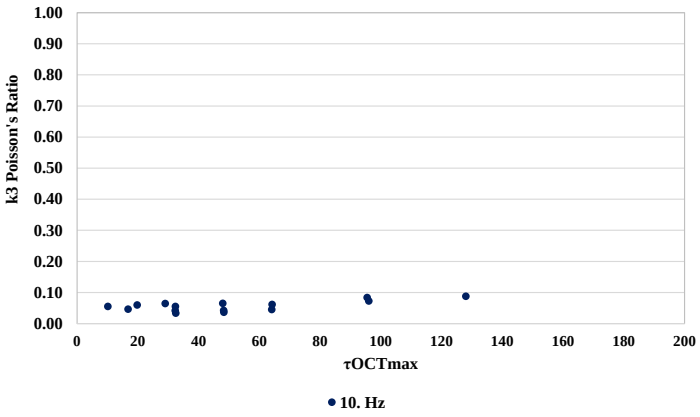

Subbase (AASHTO T307)

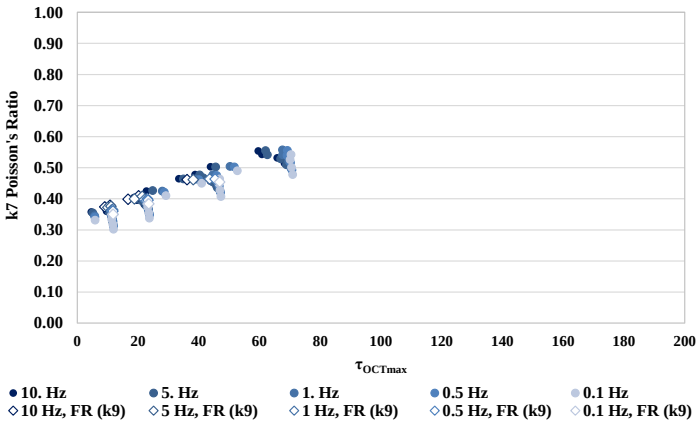

Subgrade (PSI*Materials*4D)

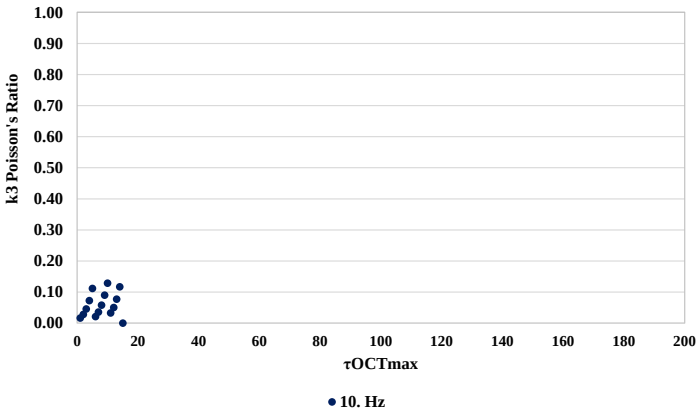

Subgrade (AASHTO T307)

During this study, when applied to typical unbound flexible pavement materials, AASHTO T307 resulted in lateral shear material sample failures during testing. Reasons for this are hypothesized to be related to shear plane layers within the sample layering and the aspect ratio of 2:1. The AASHTO T307 samples specified to be compacted in layers are considered not true continuum in composition due to introduced layer interfaces that can induce force slip planes during testing, as illustrated in Figure 13 a) through Figure 13 c) with modern construction equipment, this type of layering is also not realistic. Figure 14 illustrates the PSI*Materials*4D continuum samples of the same materials post characterization with no load induced failures visible.

Figure 13. Typical Shear Slip Plane Failures Material Samples During AASHTO T307 Triaxial Testing



a) Base b) Subbase c) Subgrade

Figure 14. PSI*Materials*4D Continuum Samples Characterized in this Study



a) Hot Mix Asphalt Concrete b) Base c) Subbase d) Subgrade

Due to the observed shear failures within the AASHTO T307 samples as illustrated in Figure 13, it is concluded that the AASHTO T307 material sample specification resulted in material stiffness modulus as well as Poisson's Ratio material properties that were considerably lower than those obtained from PSI*Materials*4D. Given the granular base, subbase as well as the subgrade materials considered in this study are common materials used successfully to construct flexible pavements, the material properties obtained from the PSI*Materials*4D appear to be more in-line with realistic material properties used for road and design analysis. As a result, AASHTO T307 may result in pavement designs that are not representative of field structural performance of flexible pavement structures.

PSI*Pave*3D Numerical Road Modelling Case Study

To illustrate the effect that material constitutive properties have on the primary response modelling of a typical flexible pavement structure, PSI*Pave*3D was used to perform 3D numerical road structural modelling using the AASHTO T307 and PSI*Materials*4D material properties. As seen in Figure 15 and Figure 16, a primary rural highway flexible pavement structure loaded by a conventional B-train was evaluated. This pavement structure was selected to illustrate the difference material constitutive properties have in a standard primary rural highway pavement. Table 1 summarizes the road structural cross sectional geometric properties used in this study.

Figure 15. Typical Rural Primary Highway Pavement Road Cross Section



Figure 16. PSI*Pave*3D Structural Cross Section Input Screen

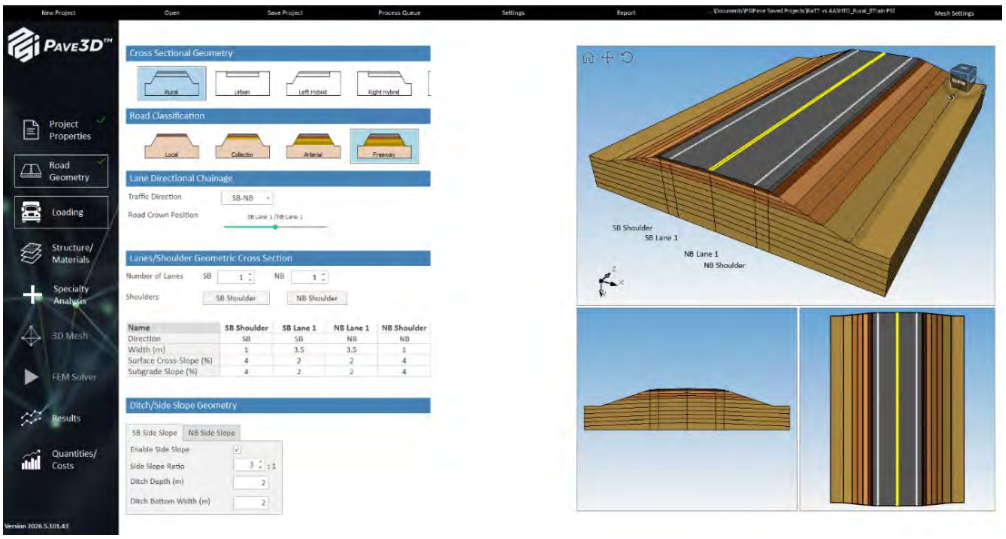

Table 1. Primary Flexible Pavement Structural Thickness used in the Structural Modelling

	SMH Specification	Layer Thickness (mm)
HMAC Surfacing	Type 1	75
Granular Base	Type 33	150
Granular Subbase	Type 8	300
Prepared Subgrade	SC	600
Subgrade	SC	3,875

Figure 17 illustrates the PSI*Pave*3D road model encoding of the pavement cross section with an 8-axle B-train loaded on a two lane highway at primary weights of 63,000 kg. Figure 18 illustrates the rural highway primary flexible pavement structure with an 8-axle B-train superimposed on one of the travelling lanes.

Primary responses used in this study to compare AASHTO T307 and PSI*Materials*4D included: peak vertical deflection, octahedral normal strain, and principal shear strain. All measures are presented with respect to depth in the road structure. As seen in Figure 19, the AASHTO T307 peak vertical deflection results with respect to depth within the road structure were considerably higher (2x) relative to those from PSI*Materials*4D. AASHTO T307 predicted peak surface vertical deflection on the threshold of failure from a peak vertical surface deflection perspective. The PSI*Materials*4D however generated vertical deflection results commonly observed from primary pavement systems.

From a principal normal and shear strain perspective as illustrated in Figure 20 and Figure 21, respectively, AASHTO T307 yielded much higher normal and shear strain states (3x) that of PSI*Materials*4D, particularly within the upper road structure. The strain state results of AASHTO T307 were found to be over the known plasticity threshold of common asphaltic concrete, granular base, subbase and subgrade soils used in this analysis.

Figure 17. 8-Axle B-Train PSI*Pave*3D Dimensions and Weights Input Screen



Figure 18. PSI*Pave*3D Primary Pavement Road Cross Section and Mesh Refinement with 8-Axle B-Train

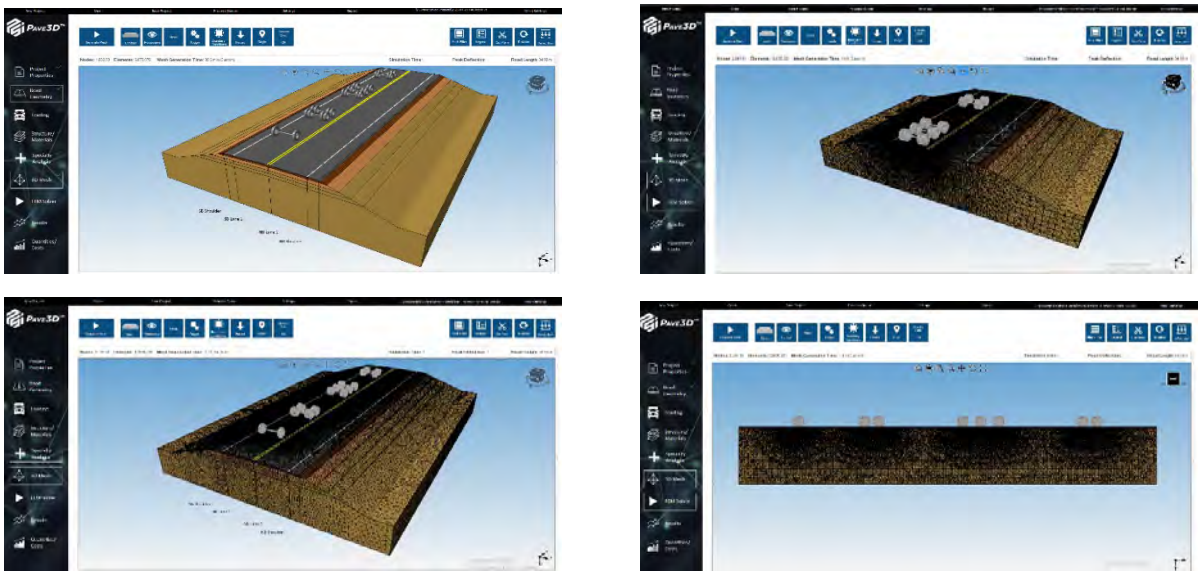

Figure 19. Peak Vertical Deflection Profile with Respect to Pavement Depth

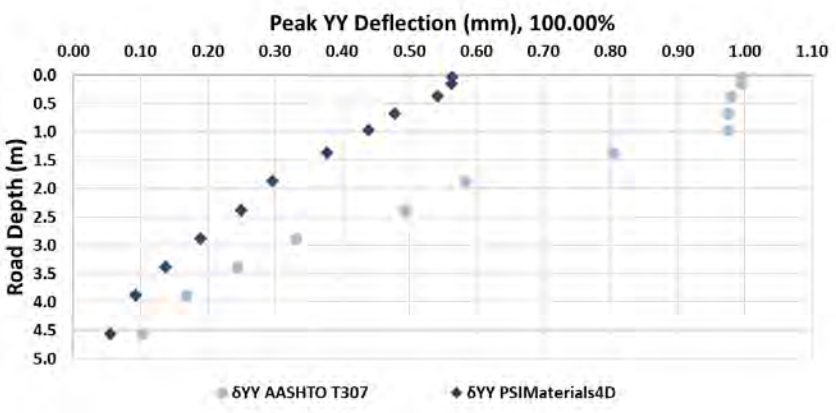

Figure 20. Peak Octahedral Orthogonal Strain Profile with Respect to Pavement Depth

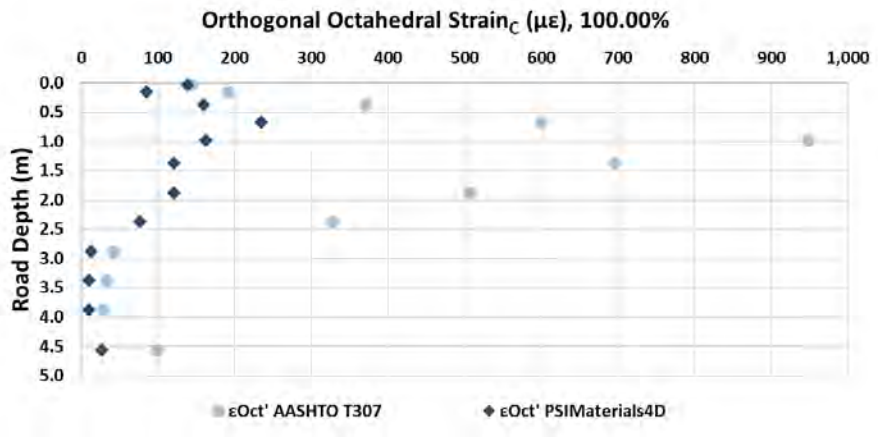

Figure 21. Principal Shear Strain Profile with Respect to Pavement Depth

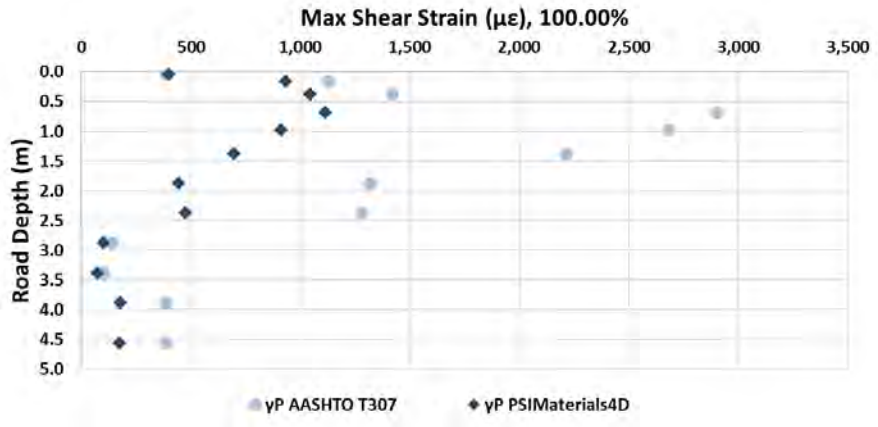

Conclusions

This study evaluated two mechanistic road material characterization protocols; AASHTO T307 and PSI*Materials*4D for purposes of mechanistic road modelling. The AASHTO T307 characterization protocols were found to not accurately capture typical *in situ* flexible pavement material constitutive behaviour for prediction of structural pavement primary response modelling. When applied to typical unbound road materials, AASHTO T307 resulted in lateral shear failure during testing. Reasons for this are hypothesized to be shear plane layers induced within the sample during compaction which is compounded with a sample height to diameter aspect ratio of 2:1. The AASHTO T307 samples are not considered true continuum in composition and therefore introduces layer interfaces that can induce force slip planes during testing.

The PSI*Materials*4D material sample protocols using feedback controlled gyratory compaction is designed to provide samples at specified density and provide a more continuum densification profile of the sample similar to that achieved in the field during construction. The material constitutive properties obtained from PSI*Materials*4D were also tested across a broader spectrum of typical rural flexible

pavement structure field stress state conditions when subjected to heavy truck load scenarios, relative to AASHTO T307.

When encoded into PSI*Pave*3D numerical road model, the AASHTO T307 material properties were found to yield primary pavement responses that were significantly greater than that obtained from PSI*Materials*4D material constitutive relations. The AASHTO T307 material properties yielded primary pavement responses that were equivalent to structural failure state of the primary flexible pavement structure which is unrealistic relative to field observations of these types of pavement structures.

In summary, the material constitutive relations obtained by AASHTO T307 do not appear to provide reasonable material constitutive properties of typical granular and soil materials commonly used for primary flexible pavement construction. The PSI*Materials*4D continuum material constitutive properties however resulted in primary pavement modelling responses that more realistically predict primary pavement structural response profiles of a typical primary flexible pavement system. In summary, the primary structural deflection and peak strain response profiles obtained from AASHTO T307 material properties were found to incorrectly predict primary pavement structural performance of flexible pavements whereas the PSI*Materials*4D material properties concurred with known structural primary response and structural performance of primary pavements constructed of the materials that were evaluated herein.

References

[1] American Association of State Highway and Transportation Officials (AASHTO) T 307-99 (2021). “Standard Test Method for Determining the Resilient Modulus of Soils and Aggregate Materials”, Standard Specifications for Transportation Materials and Methods of Sampling and Testing and AASHTO Provisional Standards, Group 3, 44th Edition, Washington, D.C. (2024).

[2] Witczak, M. “Harmonized Test Methods for Laboratory Determination of Resilient Modulus for Flexible Pavement Design, Final Report Volume I, Unbound Granular Materials”, National Cooperative Highway Research Program (NCHRP) Project No. 1-28A, Transportation Research Board, National Research Council, National Academies, Washington, D.C. (2003).

[3] Tarefder, R. “Laboratory Dynamic modulus of asphalt mixes and Resilient Modulus of Soils Throughout New Mexico for the Implementation of Mechanistic Empirical Pavement Design Guide (MEPDG), Part 2: Laboratory Resilient Modulus of Soils”. University of New Mexico. The US Department of Transportation Federal Highway Administration (2013)

[4] Ali, O. “Evaluation of the Mechanistic Empirical Pavement Design Guide (NCHRP 1- 37 A)”. Report No: UR 3002.1. National Research Council of Canada. (2005)

[5] Berthelot C., Haichert R., Berthelot J., Kalsi, A. “Comparison of AASHTO MEPDG and PSIMaterials3D Unbound Road Materials Characterization for Mechanistic Road Modelling”, Proceedings of the International Road Federation Global R2T Conference & Exhibition, Los Angeles, CA, USA (2025).

[6] Allen D., Little D., Soares R., Berthelot C. “Multi-Scale Computational Model for Design of Flexible Pavement–Part I: Expanding Multi-Scaling”, International Journal of Pavement Engineering, 18(4), 309-320 (2017).